Coarse-grained model of the nematic twist-bend phase from a stable state elastic energy

M. P. Rosseto and L. R. Evangelista
Department of Physics, Universidade Estadual de Maringá, Avenida Colombo 5790, 87020-900 Maringá, Paraná, Brazil

P. S. Simonário
Department of Physics, Universidade Estadual de Maringá, Avenida Colombo 5790, 87020-900 Maringá, Paraná, Brazil and Department of Applied Mathematics, Universidade Estadual de Campinas, Rua Sérgio Buarque de Holanda 661, 13083-859 Campinas, São Paulo, Brazil

R. S. Zola*
Department of Physics, Universidade Estadual de Maringá, Avenida Colombo 5790, 87020-900, Maringá, Paraná, Brazil and Department of Physics, Universidade Tecnológica Federal do Paraná, Rua Marcílio Dias 635, 86812-460 Apucarana, Paraná, Brazil

(Received 11 October 2019; published 3 January 2020)

The twist-bend nematic (N_{TB}) phase is a doubly degenerated heliconical structure with nanometric pitch and spontaneous bend and twist deformations. It is favored by symmetry-breaking molecular structures, such as bent dimers and bent-core molecules, and it is currently one of the burgeoning fields of liquid-crystal research. Although tremendous advances have been reported in the past five years, especially in molecular synthesis, most of its potential applications are held back by the lack of a proper and definitive elastic model to describe its behavior under various situations such as confinement and applied field. In this work we use a recently proposed stable state elastic model and the fact that the mesophase behaves as a lamellar structure to propose a mesoscopic or coarse-grained model for the N_{TB} phase. By means of standard procedures used for smectic and cholesteric liquid crystals, we arrive at a closed-form energy for the phase and apply it to a few situations of interest. The predicted compressibility for several values of the cone angle and the critical field for field-induced deformation agree well with recent experimental data.

DOI: 10.1103/PhysRevE.101.012702

I. INTRODUCTION

Despite having remarkable characteristics, such as spontaneous twist and bend deformations, and presenting a doubly degenerated heliconical state with a nanometric pitch, the twist-bend nematic (N_{TB}) phase has drawn considerable attention not only for its unique features but also for the possibilities of new applications. From the experimental point of view, the existence of this mesophase has been reported in achiral bent dimers [1–6], trimers [7], rigid bent-core materials [8], and chiral dimers [9] and is quickly escalating to several other types of molecular shape that present some kind of bent structure [10]. A few publications have been dedicated to the probe and characterization of the mesophase [11–17] and also to the development of applications of the materials forming the N_{TB} phase [18–21].

Many of the potential applications, however, lose their strength without a suitable model to describe the phase, especially its elasticity. In fact, several of the recent studies still use the Frank energy and the corresponding elastic constants to describe or extrapolate their data. Although the N_{TB} phase was first predicted theoretically years ago [22–24], the recently proposed models for the N_{TB} elasticity are yet to prove their strength. Among them, Frank- and Landau-like descriptions [25–29] and molecular approaches have been proposed [30], but a direct comparison of such models with experimental data has not been made. It has also been argued that flexoelectricity is responsible for the N_{TB} stability [31–33], but recent experimental evidence suggests flexoelectricity cannot explain, for example, the large compression modulus measured [33]. On the other hand, due to the heliconical pitch (repeating itself structure), the N_{TB} phase might be viewed as a pseudolayer medium [14,17]. It is therefore convenient to employ the coarse-graining method to model the mesophase in terms of pseudolayers' deformations, which occur at length scales much larger than the pitch, rather than in terms of the molecular director. Challa *et al.* [14] used a smectic coarse-grained energy to interpret results of N_{TB} subjected to a strong magnetic field. Meyer and Dozov [34,35] suggested that the N_{TB} phase may be described as an effective chiral smectic-*A* phase. Parsouzi *et al.* [12] also presented a coarse-grained model which might be indirectly connected with the smectic-*A* phase. Shiyanovskii *et al.* [36], on the other hand, presented a coarse-grained energy that is derived from a nematic double-well potential, introducing the dependence on the cone angle, which does not occur in the smecticlike models.

In this paper, we use the recently proposed energy [26] to derive its coarse-grained version for the N_{TB} phase. The

*Corresponding author: rzola@utfpr.edu.br

nematic energy used here corresponds to the stable state of a quadratic elastic theory formed with the symmetry elements of the phase. The procedure is the coarse-grained approach employed to the smectic and cholesteric phases [37–39]. We show that the bulk modulus calculated with our model agrees with recently published experimental data. We also calculate other parameters of interest and examine the behavior of the system under the action of an external field, in order to obtain the thresholds for the field-induced deformations.

II. THEORY

The elastic continuum theory for the nematic phase has been extended to describe the $N_{\rm TB}$ phase, as recently published in Ref. [26]. In summary, the helical axis is defined and represented by a new director field $\mathbf{t}$, around which the molecular director $\mathbf{n}$ precesses uniformly. This new element of symmetry was included in Ref. [26]. To describe the $N_{\rm TB}$ configuration, the nematic director can be expressed as

$$\mathbf{n} = \sin\theta[\cos\phi(\mathbf{u}_x) + \sin\phi(\mathbf{u}_y)] + \cos\theta(\mathbf{u}_z), \tag{1}$$

where θ is the cone angle and ϕ is the azimuthal angle. Notice that $\nabla\phi = \mathbf{q}$ gives the wave vector of the $N_{\rm TB}$ phase. Here $(\mathbf{u}_x, \mathbf{u}_y, \mathbf{u}_z)$ represent the fixed unit vectors along the Cartesian axis. Following the procedure as presented in Ref. [40], the elastic energy density can be reduced as

$$\begin{aligned} f = f_1 &- \tfrac{1}{2}\eta(\mathbf{n}\cdot\mathbf{t})^2 + \kappa_2\,\mathbf{n}\cdot\nabla\times\mathbf{n} \\ &+ \tfrac{1}{2}K_{22}(\mathbf{n}\cdot\nabla\times\mathbf{n})^2 + \tfrac{1}{2}K_{33}(\mathbf{n}\times\nabla\times\mathbf{n})^2 \\ &+ \nu_4(\mathbf{t}\times\nabla\times\mathbf{n})^2, \end{aligned} \tag{2}$$

where K_{22} and K_{33} are the Frank twist and bend elastic constants, respectively. Also, there are two new elastic parameters here: ν_4, a new elastic constant associated with bend renormalization, and the pseudoscalar κ_2. Before we describe the physical meaning of the latter, it is important to note that, as previously shown [26], the stability analysis (Hessian determinant) dictates that there exists a critical value of κ_2 for the existence of the $N_{\rm TB}$ phase. In other words, it must be larger than $\kappa_c = \pm\eta/q^*$, where η represents the coupling between $\mathbf{n}$ and $\mathbf{t}$, and q^* is the wave vector of the phase; otherwise, the $N_{\rm TB}$ structure is not stable. We stress the relation between κ_2 and q^* on showing, according to Ref. [26], how the $N_{\rm TB}$ cone angle is stabilized:

$$\sin^2\theta^* = -\frac{K_{33} + 2\nu_4 \mp \kappa_2/q^*}{K_{22} - K_{33}}. \tag{3}$$

Thus, the sign of q^*, indicating a right- or left-handed twist, also indicates the sign of κ_2, which, on the other hand, always results in the same tilt angle [26]. Such a relation between the wave vector and κ_2 indicates that the rotation direction is dictated by the molecular shape of the molecules rather than macroscopic chirality, so both rotation senses are equally likely in the $N_{\rm TB}$ phase. Hence, we interpret that κ_2 quantifies the tendency of the molecules to twist: It is different from zero (i) for chiral molecules in the cholesteric limit [38] and (ii) for achiral molecules with heliconical structure [26].

The use of a coarse-graining approach has been proposed to present a different view on the elastic continuum theory of the $N_{\rm TB}$ phase. Since the optical wavelength is larger than the heliconical structure, light-scattering experiments rely on the mesoscopic scale deformations. In short, the coarse-graining theory is an attempt to express the elasticity of the $N_{\rm TB}$ phase in terms of the pseudolayers deformations, supposedly to occur at longer than light wavelength scales, rather than using classical distortions in terms of the director $\mathbf{n}$. Figure 1 illustrates the mobile system of coordinates, discussed below, and the deformation of the equipotential surfaces; in the close-up region, the arrows represent the helical axis $\mathbf{t}$. Based on the pseudolayer structure and since the azimuthal angle average, described by $\langle\nabla\phi\rangle$, varies slowly in space [39], it expresses the coarse-grained director $\mathbf{t}$ as several heliconical periods in a spatial region (Fig. 1).

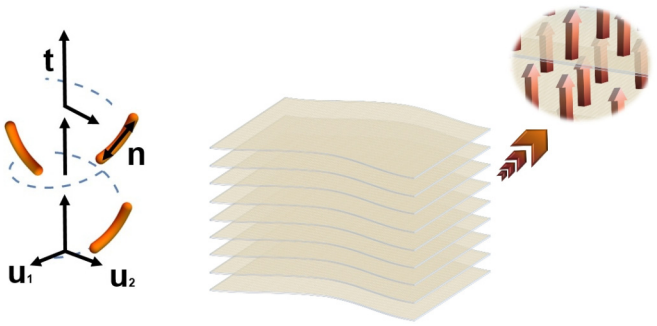

FIG. 1. Twist-bend nematic phase represented by the molecular arrangement and the augmented scale, in terms of the pseudolayer structure.

To begin, we should note that ϕ is a fast-changing function, as it varies over the pitch length scale [36]. However, we remark that $\langle\nabla\phi\rangle$ is a slowly changing field, when the average is made over the pitch distance. Also, let us consider that the fields $\mathbf{t}$ and θ are spatial variables, in addition to ϕ. This lead us to the most general expressions of the spatial variation of $\mathbf{n}$ and, consequently, the coarse-grained energy. Let us set a new Cartesian frame $(\mathbf{u}_1, \mathbf{u}_2, \mathbf{u}_3)$, with $\mathbf{u}_3 \equiv \mathbf{t}$, which is variable in space and describes the orientation of the local director [37]. In this framework, the director can be rewritten as

$$\mathbf{n} = \sin\theta[\cos(\phi)\mathbf{u}_1 + \sin(\phi)\mathbf{u}_2] + \cos(\theta)\mathbf{t} \tag{4}$$

and its spatial variation is such that

$$\begin{aligned} \nabla\mathbf{n} = &-\cos\theta(\mathbf{u}_1\otimes\mathbf{c}_1 + \mathbf{u}_2\otimes\mathbf{c}_2) \\ &+ \sin\theta\{\mathbf{t}\otimes[\cos(\phi)\mathbf{c}_1 + \sin(\phi)\mathbf{c}_2]\} \\ &- \sin\theta(\mathbf{t}\otimes\nabla\theta) + \cos\theta[\cos(\phi)\mathbf{u}_1 + \sin(\phi)\mathbf{u}_2]\otimes\nabla\theta \\ &+ \sin\theta[-\sin(\phi)\mathbf{u}_1 + \cos(\phi)\mathbf{u}_2]\otimes\nabla\phi. \end{aligned} \tag{5}$$

In Eq. (5) we used the connectors $\mathbf{c}_1$ and $\mathbf{c}_2$ to write [36,37]

$$\nabla\mathbf{u}_i = \mathbf{t}\otimes\mathbf{c}_i, \quad \nabla\mathbf{t} = -\mathbf{u}_1\otimes\mathbf{c}_1 - \mathbf{u}_2\otimes\mathbf{c}_2, \tag{6}$$

where $i = 1, 2$. One may find a more detailed explanation about connectors and their generalizations in Refs. [36,37]. The coarse-grained energy is found by (i) inserting Eqs. (4) and (5) into Eq. (2), with the aid of Eq. (6); (ii) averaging f over the rapid field ϕ; and (iii) minimizing $\langle f\rangle$ over $\nabla\phi$, which

gives

$$\langle\nabla\phi\rangle_\perp = \frac{2K_{22}\sin 2\theta}{4K_{33}\sin^4\theta + K_{22}\sin^2 2\theta}(\nabla\theta\times\mathbf{t}) + \frac{(K_{22}-K_{33})\sin^2 2\theta}{4K_{33}\sin^4\theta + K_{22}\sin^2 2\theta}(\nabla\times\mathbf{t})_\perp,$$

$$\langle\nabla\phi\rangle\cdot\mathbf{t} = q_{t0} - \frac{2K_{22}-K_{33}+2\nu_4-(K_{22}-K_{33})\sin^2\theta}{2[(K_{22}-K_{33})\sin^2\theta + K_{33}+2\nu_4]}\times(\mathbf{t}\cdot\nabla\times\mathbf{t}), \tag{7}$$

that is, the perpendicular and parallel (with respect to $\mathbf{t}$) components of $\nabla\phi$'s average, respectively, which minimizes $\langle f\rangle$.

In Eq. (7) we used $\langle\nabla\phi\rangle\cdot\mathbf{t} = q_t$; also, $\langle\nabla\phi\rangle\cdot\mathbf{u}_1 = q_1$ and $\langle\nabla\phi\rangle\cdot\mathbf{u}_2 = q_2$, which are both used to write $\langle\nabla\phi\rangle_\perp$. The equilibrium state that minimizes the free energy of the system leads to q_{10}, q_{20}, and q_{t0}, the optimum twist considering each possible distorted direction, analogous to the classic elastic theory for the natural wave vector.

The last step to find the coarse-grained energy is replacing Eq. (7) in $\langle f\rangle$, which results in

$$\begin{aligned}F_{\rm CG} = {}& \alpha + \frac{1}{2}B\left(\frac{p_z}{p_{z0}}-1\right)^2 + \frac{1}{2}Cq_\perp^2 \\ & + \frac{1}{2}\alpha_1(\nabla\cdot\mathbf{t})^2 + \frac{1}{2}\alpha_2(\mathbf{t}\cdot\nabla\times\mathbf{t})^2 \\ & + \frac{1}{2}\alpha_3(\mathbf{t}\times\nabla\times\mathbf{t})^2 + \alpha_4\nabla\cdot(\mathbf{t}\nabla\cdot\mathbf{t}+\mathbf{t}\times\nabla\times\mathbf{t}) \\ & + \beta_1(\nabla\theta\times\mathbf{t})^2 + \beta_2(\nabla\theta\cdot\mathbf{t})^2 \\ & + \beta_3(\nabla\cdot\mathbf{t})(\nabla\theta\cdot\mathbf{t}) + \beta_4\nabla\theta\cdot(\mathbf{t}\times\nabla\times\mathbf{t}).\end{aligned} \tag{8}$$

Here B and C represent, respectively, compressions along and perpendicular to $\mathbf{t}$; the elastic constants α_i and β_i, with $i = 1$–4, are related to deformations of $\mathbf{t}$ and θ, respectively. By comparison with the Frank free energy, we associate each term in Eq. (8) with one kind of deformation: α terms are related to distortions of $\mathbf{t}$ and the β terms to variations of θ. Clearly, the physical meaning of the α constants is related to classical $\mathbf{t}$ distortions (splay, twist, and bend), whereas the constants β represent a new set of elastic parameters [36]. Such parameters are written in terms of the molecular constants as

$$\begin{aligned}\alpha &= f_0 - \tfrac{1}{2}\left[\eta\cos^2\theta + Bq_{t0}^2 + C\left(q_{10}^2+q_{20}^2\right)\right], \\ B &= q_t^2[(K_{22}-K_{33})\sin^2\theta + K_{33}+2\nu_4]\sin^2\theta, \\ C &= \tfrac{1}{4}[K_{22}+K_{33}+(K_{22}-K_{33})\cos 2\theta]\sin^2\theta\end{aligned} \tag{9a}$$

for the "ground-state" and compression terms,

$$\begin{aligned}\alpha_1 &= \frac{1}{8}[4(K_{33}+2\nu_4)+(K_{22}-K_{33})\sin^2\theta]\sin^2\theta, \\ \alpha_2 &= \frac{\sin^2\theta}{2}\left[2\nu_4+K_{33}+\tfrac{3}{4}(K_{22}-K_{33})\sin^2\theta\right]+K_{22}\cos^2\theta, \\ \alpha_3 &= \frac{1}{2}(K_{33}+4\nu_4+K_{22})\sin^2\theta\cos^2\theta+(K_{33}+2\nu_4)\cos^4\theta, \\ \alpha_4 &= \frac{\sin^2\theta}{8}(-K_{22}-3K_{33}-8\nu_4)+\frac{\sin^2\theta}{8}(K_{22}-K_{33})\cos 2\theta\end{aligned} \tag{9b}$$

for the parameters related to $\mathbf{t}$ and $\nabla\mathbf{t}$, and finally

$$\begin{aligned}\beta_1 &= \tfrac{1}{4}[K_{22}+(K_{33}+12\nu_4)\sin^2\theta], \\ \beta_2 &= \tfrac{1}{2}K_{33}\cos^2\theta+\nu_4(2-\cos 2\theta), \\ \beta_3 &= -\tfrac{1}{4}(K_{33}+2\nu_4)\sin 2\theta, \\ \beta_4 &= -\tfrac{1}{4}(K_{22}+K_{33}+2\nu_4)\sin 2\theta\end{aligned} \tag{9c}$$

for the constants related to $\nabla\theta$.

Here $(q_t-q_{t0})^2 = q_t^2(p_z/p_{z0}-1)^2$, where q_{t0} and q_t are the natural and the $\mathbf{t}$ direction wave vector of the $N_{\rm TB}$ phase, respectively (p_z and p_{z0} are the periods of the $N_{\rm TB}$ phase in the distorted and in the equilibrium structure, respectively). Likewise, $q_\perp^2 = (q_1-q_{10})^2+(q_2-q_{20})^2$ represents the wave vector perpendicular to the director $\mathbf{t}$. Also, we have neglected any natural twist of $\mathbf{t}$ in the expressions (9). We stress that Eq. (8) is the most general form of the coarse-grained energy derived from Eq. (2), including not only distortions in the director field $\mathbf{t}$, but also variations of the cone angle θ, represented by the elastic constants in Eq. (9c). However, for simplicity, we will assume from now on that θ is uniform across the cell. Although it is not clear yet how much θ would change as the pseudolayers change, recent experimental results have only measured changing values of θ as the temperature changes (see, for instance, Ref. [41]). Here we will only study the effect of the cone angle on the elastic constants of the coarse-grained model. Studies involving how the terms in Eq. (9c) behave appear to be an interesting exercise and worth pursuing in the future.

The energy can be further simplified if we notice that $q_\perp$ does not contribute to the free energy because it corresponds to the uniform rotations around the pseudolayers [38,42]. Considering the two assumptions above, we may write

$$\begin{aligned}F_{\rm CG} = {}& \alpha + \frac{1}{2}B\left(\frac{p_z}{p_{z0}}-1\right)^2 + \frac{1}{2}\alpha_1(\nabla\cdot\mathbf{t})^2 \\ & + \frac{1}{2}\alpha_2(\mathbf{t}\cdot\nabla\times\mathbf{t})^2 + \frac{1}{2}\alpha_3(\mathbf{t}\times\nabla\times\mathbf{t})^2 \\ & + \alpha_4\nabla\cdot(\mathbf{t}\nabla\cdot\mathbf{t}+\mathbf{t}\times\nabla\times\mathbf{t}).\end{aligned} \tag{10}$$

Moreover, the term associated with α_4 is a surface contribution and therefore can be neglected [43]. In an idealized experiment of equidistant layers, it is possible to assume that $\mathbf{t}\parallel\mathbf{q}$ and therefore $\nabla\times\mathbf{t} = 0$, which reduces the coarse-grained energy to

$$F_{\rm CG} = \alpha + \frac{1}{2}B\left(\frac{p_z}{p_{z0}}-1\right)^2 + \frac{1}{2}\alpha_1(\nabla\cdot\mathbf{t})^2. \tag{11}$$

According to Ref. [38], the coarse-grained energy for cholesterics is

$$F_{\rm chol} = \frac{1}{2}B_{\rm eff}\left(\frac{P}{P_0}-1\right)^2 + \frac{1}{2}K_{\rm eff}(\nabla\cdot\mathbf{d})^2, \tag{12}$$

in which P is the pitch of the phase, P_0 is the equilibrium pitch, and $\mathbf{d}$ is a unit vector normal to the layers. Therefore, a direct comparison between Eqs. (12) and (11) suggests that $\alpha_1 = K_{\rm eff}$ and $B = B_{\rm eff}$; a similar correlation has been made in Ref. [38]. Hence, α_1 can be thought of as the effective elastic constant and B as the bulk modulus of the $N_{\rm TB}$ phase. Note that B takes the same form as the cholesteric phase

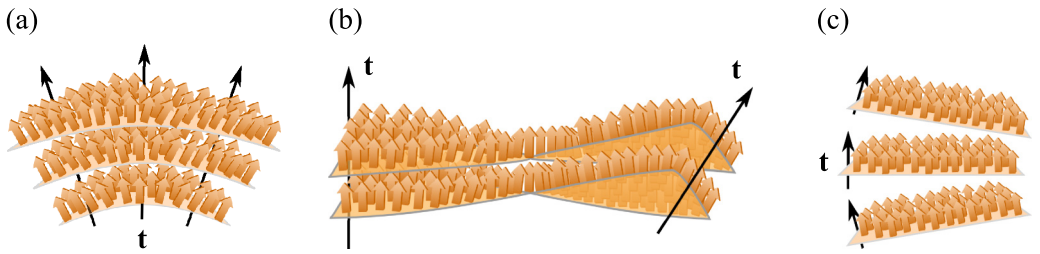

FIG. 2. (a) Splay, (b) twist, and (c) bend of the director field **t**, related to K_{eff}, α_2, and α_3, respectively. The pseudolayers' distortions and separations are exaggerated for didactic purposes.

(dependence on the wave vector and elastic constants), which is expected since both coarse-grained models are based on a similar procedure of leaving from a stable state elastic energy to an augmented form of the energy. Indeed, if $\nu_4 = 0$ and $\theta = \pi/2$ (cholesteric limit), we arrive at $B = K_{22}q_0^2$ ($q_t = q_0$), as previously shown [40]. Furthermore, by taking the same limits and assuming that the twist deformation drops out [see Eq. (9b)], the cholesteric limit ($\alpha_1 = K_{\text{eff}} = 3K_{33}/8$) [38] is again achieved. This association of α_1 and K_{eff} is quite clear once we consider that a splay in **t** represents bending the pseudolayers, which in the coarse-grained theory is associated with the bend elastic constant of the Frank-Oseen free energy [43]. In conclusion, the coarse-grained elastic energy can be written as

$$F_{\text{CG}} = \alpha + \frac{1}{2}B_{\text{eff}}\left(\frac{p_z}{p_{z0}} - 1\right)^2 + \frac{1}{2}K_{\text{eff}}(\nabla \cdot \mathbf{t})^2 + \frac{1}{2}\alpha_2(\mathbf{t}\cdot\nabla\times\mathbf{t})^2 + \frac{1}{2}\alpha_3(\mathbf{t}\times\nabla\times\mathbf{t})^2 + \alpha_4\nabla\cdot(\mathbf{t}\nabla\cdot\mathbf{t} + \mathbf{t}\times\nabla\times\mathbf{t}). \quad (13)$$

For the purposes of clarifying our understanding of the elastic terms in Eq. (13) and comparing them to the Frank free energy for uniaxial nematics, the illustration shown in Fig. 2 exhibits the distortions of **t** related to $K_{\text{eff}} \equiv \alpha_1$, α_2, and α_3. From now on, all comparisons with experimental data, and applications on external perturbation problems, are performed using Eq. (13).

A. Bulk modulus

As discussed in the preceding section, our model allows the calculation of the so-called bulk modulus or compressibility of the pseudolayers using only the symmetry elements permitted in the N_{TB} phase. Further, B, as here described, has been the subject of some discussion in recent publications, mainly due to some observed discrepancy between measured and predicted data. There are data available in the literature for at least two different materials forming the N_{TB} phase: a 20 mol % methylene linked dimer 1″, 9″-bis(4-cyano-2′-fluorobiphenyl-4′-yl)nonane [KA(0.2)] [44] and 1″, 7″-bis(4-cyanobiphenyl-4′-yl)heptane (CB7CB) [45]. For the KA(0.2) material, the compressibility is estimated from flow measurements to be $B \approx 2$ kPa. For CB7CB, B was obtained with the aid of piezoelectric ceramics and measuring the mechanical transfer function; it was found to be roughly 200 kPa near the nematic transition. From Eq. (8), the compressibility can be calculated once the following parameters are known: $q = 2\pi/p$ (p is the pitch of the N_{TB} phase), the cone angle θ, K_{22}, K_{33}, and ν_4. Based on the nematic phase, the elastic constants [1,3,46] can be measured and extrapolated to the N_{TB} phase. Furthermore, both the pitch length and the cone angle have been measured for both materials in several publications. On the other hand ν_4 was recently introduced in Ref. [26] but has not yet been measured. Nonetheless, its value can be estimated. As demonstrated in Ref. [40], it lies within the bounded interval $-K_{33}/2 < \nu_4 < (K_{22} - K_{33})/2$. Hence, we propose the value of ν_4 in this quite small range which best adjusts the values of B found in the literature for each material.

First, for KA(0.2), we used $p = 10.5$ nm [47] of pitch and $\theta = 15^\circ$ [47]. The elastic constants, as obtained in Ref. [1], are approximately $K_{22} = 5$ pN and $K_{33} = 1$ pN. Also, we used $\nu_4 = -0.49K_{33}$. With these parameters and by using B given in Eq. (9a), we get $B \approx 10^3$ Pa, in reasonable agreement with the rheological study in [44]. Second, for CB7CB we used $K_{22} = 5$ pN, $K_{33} = 0.3$ pN, and $p = 8.05$ nm [3,46]. However, for this material, the cone angle depends drastically on temperature. Reference [41] reports a strong variation of θ, ranging from 9° (near the nematic transition) to over 35° (low temperature), deep in the N_{TB} phase. We find that $\nu_4 = 0.34(K_{22} - K_{33})$ gives the best results for CB7CB. Deep in the N_{TB} phase, that is, $\theta \approx 35^\circ$, we obtain $B \approx 10^6$ Pa, similar to what has been measured by Gorecka *et al.* [45]. On the other hand, near the nematic transition $\theta \approx 10^\circ$ results in $B \approx 10^4$ Pa, roughly 100 times smaller than the values measured for smectic phases and in agreement with the predictions of the flexoelectric model [12]. Notice that for this calculation, while we assumed that the pitch of CB7CB does not change considerably with temperature [11], the values of the elastic constants are the ones measured for the nematic phase near the transition. Thus, the values used for ν_4 might somehow be compensating for the lack of precise values of Frank elastic constants, since they are the only data not derived from experimental results. Nonetheless, our results are in good agreement with recently measured values of B and with predicted values of the flexoelectric model, depending on the cone angle. Figure 3 reveals the volatility of B against the cone angle, which changes expressively within a few degrees.

With the coarse-grained free energy (13), we can calculate the penetration length $\lambda = \sqrt{K_{\text{eff}}/B_{\text{eff}}}$, which describes the distortions relaxation length [43]. According to Eq. (10),

$$\lambda = \frac{1}{2q_t}\sqrt{\frac{4(K_{33} + 2\nu_4) + (K_{22} - K_{33})\sin^2\theta}{2[K_{33} + 2\nu_4 + (K_{22} - K_{33})\sin^2\theta]}}, \quad (14)$$

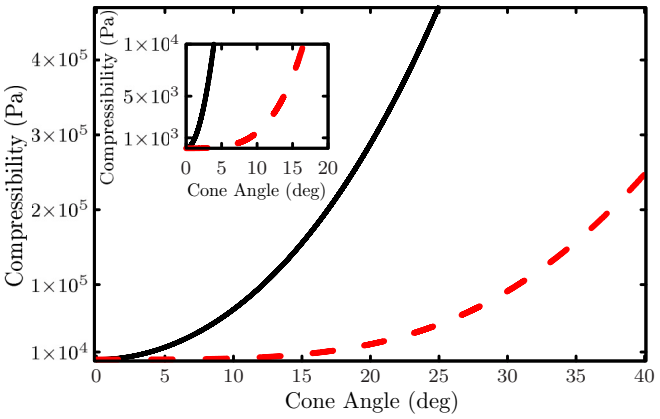

FIG. 3. Cone angle in the N_{TB} as a function of the compressibility. The black solid line exhibits the variation of CB7CB, while the red dashed line is the measure of KA(0.2).

which, by using the parameters of CB7CB, we find $\lambda \approx 0.62/q_t$ [$\lambda \approx 0.38/q_t$ when using the parameters of KA(0.2)], which is smaller than the N_{TB} period, which consequently indicates a slow variation of $\mathbf{t}$, as predicted in coarse-grained theories [12,34,39,43].

It is also helpful to observe how the elastic constants in Eq. (13) change while the cone angle varies from 0 to $\pi/2$ as described by Eq. (9b) (see Fig. 4 for CB7CB). The parameters K_{eff}, α_2, and α_3 are bulk elastic constants representing the splay, twist, and bend of $\mathbf{t}$, respectively, and α_4 is a surface term. We note that K_{eff} is one order of magnitude smaller than α_2 and α_3 for the values of θ, typically measured within the N_{TB} phase ($10^\circ \leqslant \theta \leqslant 35^\circ$), suggesting that it is easier to promote splay of $\mathbf{t}$ (bending of the pseudolayers) than other distortion. Indeed, other distortions of $\mathbf{t}$ could potentially require changes in the pseudolayer spacing, which costs elastic energy and could indicate changes in the cone angle distribution across the cell, so the whole model would be necessary to represent such distortions. From Fig. 4 we observe that K_{eff}'s magnitude becomes closer to the other elastic constants only for a large cone angle, where also the

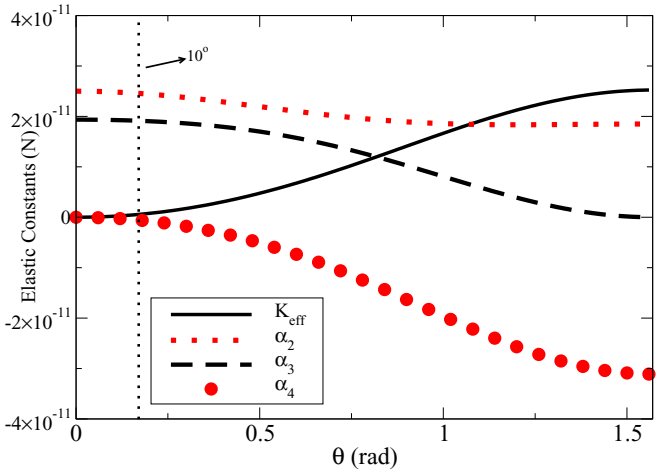

FIG. 4. Elastic constants from Eq. (13) vs θ when the physical parameters of CB7CB are used.

bulk modulus grows (Fig. 3), meaning that the splay of $\mathbf{t}$ could still be favorable since changing layer spacing becomes more difficult for large values of B. Finally, we notice that the surface term is negative even for small values of the cone angle, which could be the reason for the periodic structure (optical stripes) often observed in the N_{TB} phase [48].

B. Magnetic field

In order to consider a specific example and to demonstrate a practical application of the model here proposed, we study the effect of an external magnetic field applied to the N_{TB} structure. To do this, we first need to compute the coupling between the applied field and $\mathbf{t}$. We start by writing the field energy in terms of the director $\mathbf{n}$ as

$$f_{\mathrm{magnetic}} = -\frac{1}{2}\frac{\chi_a}{\mu_0}(\mathbf{H}\cdot\mathbf{n})^2,$$

in which $\mathbf{H}$ is the applied magnetic field, χ_a is the diamagnetic susceptibility, and μ_0 is the permeability of free space. By using the coarse-graining procedure, similar to what has been done in Ref. [36], we find

$$F_{\mathrm{magnetic}} = -\frac{1}{2}\frac{\chi_a}{\mu_0}\langle[\sin\theta\cos\phi(\mathbf{H}\cdot\mathbf{u}_1) + \sin\theta\sin\phi\,(\mathbf{H}\cdot\mathbf{u}_2) + \cos\theta(\mathbf{H}\cdot\mathbf{t})\,]^2\rangle.$$

Since $(\mathbf{H}\cdot\mathbf{u}_1)^2 + (\mathbf{H}\cdot\mathbf{u}_2)^2 = H^2 - (\mathbf{H}\cdot\mathbf{t})^2$, in the mesoscopic distortions limit, we define the magnetic energy as

$$F_{\mathrm{magnetic}} = -\frac{1}{2}\frac{\chi_a}{\mu_0}\left[\frac{1}{2}(3\cos^2\theta - 1)\right](\mathbf{H}\cdot\mathbf{t})^2 + \frac{1}{4}\frac{\chi_a}{\mu_0}H^2\sin^2\theta. \tag{15}$$

The second term on the right-hand side does not depend on $\mathbf{t}$, so it can be discarded. Moreover, note that Eq. (15), when $\mathbf{H} \parallel \mathbf{t}$, returns to the magnetic contribution for the smectic phase as used in Ref. [14]. Considering $\mathbf{t} \parallel \mathbf{q}$, the coarse-grained elastic energy, Eq. (13) is simplified as Eq. (11) and the bulk energy density in the presence of the magnetic field is

$$F = F_{\mathrm{CG}} + F_{\mathrm{magnetic}} = \alpha + \frac{1}{2}B\left(\frac{p_z}{p_{z0}} - 1\right)^2 + \frac{1}{2}K_{\mathrm{eff}}(\nabla\cdot\mathbf{t})^2 - \frac{1}{2}\chi_{\mathrm{TB}}(\mathbf{H}\cdot\mathbf{t})^2,$$

where $\chi_{\mathrm{TB}} = \chi_a(3\cos^2\theta - 1)/2\mu_0$ is the effective diamagnetic susceptibility in the N_{TB} phase. Note, therefore, that the magnetic anisotropy is cone angle dependent; in other words, if the cone angle is smaller than 54.7°, a value known as the magic angle, the energy is a minimum if $\mathbf{H} \parallel \mathbf{t}$, but once the cone angle becomes larger than 54.7°, $\mathbf{H}$ must be perpendicular to $\mathbf{t}$.

We now choose a geometry, as in Fig. 5, in which the sample is bounded by two substrates separated by a distance d, the field is perpendicular to $\mathbf{t}$, $\mathbf{H} = H\mathbf{u}_3$, and $\mathbf{t} = (0, \cos\gamma, \sin\gamma)$, where $\gamma = \gamma(z)$ is the tilt angle of $\mathbf{t}$. Therefore, we get

$$F = \alpha + \frac{1}{2}B\left(\frac{p_z}{p_{z0}} - 1\right)^2 + \frac{1}{2}K_{\mathrm{eff}}\cos^2\gamma\,\gamma'^2 + \frac{1}{2}\alpha_3\sin^2\gamma\,\gamma'^2 - \frac{1}{2}H^2\chi_{\mathrm{TB}}\sin^2\gamma, \tag{16}$$

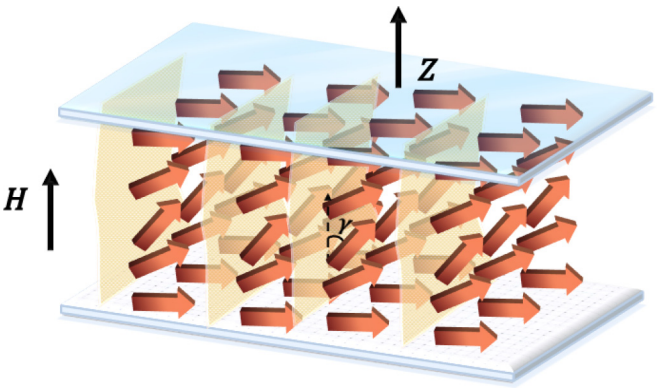

FIG. 5. Illustration of the twist-bend nematic phase with a magnetic field perpendicular to the helical axis.

with $\gamma' = d\gamma/dz$. After applying the Euler-Lagrange equation to Eq. (16), we obtain

$$(K_{\rm eff} - \alpha_3)\gamma^2 \sin\gamma\cos\gamma - H^2\chi_{\rm TB}\sin\gamma\cos\gamma - (K_{\rm eff}\cos^2\gamma + \alpha_3\sin^2\gamma)\gamma'' = 0, \quad (17)$$

in which $\gamma'' = d^2\gamma/dz^2$.

We now consider small distortions of **t** [49] in such a way that the tilt angle γ is small, and hence Eq. (17) acquires the form

$$K_{\rm eff}\gamma'' + H^2\chi_{\rm TB}\gamma = 0. \quad (18)$$

Equation (18) is simply solved as

$$\gamma(z) = A_0\cos\left(\frac{z}{\xi_M}\right) + B_0\sin\left(\frac{z}{\xi_M}\right),$$

with $1/\xi_M^2 = \chi_{\rm TB}H^2/K_{\rm eff}$. We now impose the boundary condition $\gamma(0) = \gamma(d) = 0$, which states that **t** is fixed at the boundaries. A word of caution is in order here. How the director **t** anchors at solid substrates is not well understood at this moment, since there is no clear transition from the molecular anchoring of the director **n** to the coarse-grained director **t** [36]. One possible approach would be the use of an "intrinsic" anchoring energy, as has been used in smectic-*A* and cholesteric materials [50,51]. However, our proposed boundary conditions may be understood in analogy with smectics, whose layers often orient parallel or perpendicular to the bounding substrates (an external field can also be used to aid alignment) [51]. Since we are interested in the small-angle regime, that is, distortions should occur only near the center of the sample (bulk effect), the fixed boundary condition still holds. Therefore, we obtain

$$\gamma(d) = B_0\sin\left(\frac{d}{\xi_M}\right) = 0,$$

resulting in a critical field as

$$H_c = \frac{\pi}{d}\sqrt{\frac{2\mu_0 K_{\rm eff}}{\chi_a(3\cos^2\theta - 1)}}.$$

We first notice that this field is similar to that in Ref. [14], found to explain the texture transition of the $N_{\rm TB}$ phase under high magnetic fields. By using the same parameters as in calculating the bulk modulus B for CB7CB, for $d = 2$ μm and $\chi_a \approx 10^{-6}$, we find $H_c \approx 1$ T. Note that this H_c is of the same order of magnitude as some of the results found in Ref. [14]. However, our calculations report on changes in the pseudolayers in a quite distinct configuration, where the layers are well oriented and the director **t** is perfectly oriented parallel to the bounding substrates. In Ref. [14], however, the fields were used to inhibit the optical stripes present in the $N_{\rm TB}$ phase. Clearly, a more precise description of the anchoring at the substrates, as well as a proper identification of how the pseudolayers orient when optical stripes are observed, is necessary. These topics, among others, should be explored in the future in order to make a better comparison with experimental results.

III. CONCLUSION

We have derived a coarse-grained model for the $N_{\rm TB}$ phase using a stable state free energy as the starting point. Our derivation, which focuses on pseudolayer distortions (director field **t**) rather than the director **n**, permits the calculation of possible deformations in the $N_{\rm TB}$ structure, as well as the elastic constants related to such deformations, and its dependence on the Frank elastic constants and the cone angle. In particular, our model recovers the cholesteric free energy when the correct limits are considered; it predicts the values of the bulk modulus of the $N_{\rm TB}$ phase depending on the cone angle, with calculated values close to results recently published in the literature. We also showed an example of an applied magnetic field and the prediction for the critical field for a particular configuration. The model presented here allows for simple use and direct connection with the elastic molecular model, thus allowing a facile method for measuring some of the elastic parameters that seemed to be inaccessible with Frank-like models. Hopefully, models such as the one presented here will allow further discoveries and applications of this remarkable nematic mesophase.

ACKNOWLEDGMENTS

The authors are grateful for financial support from the National Council for Scientific and Technological Development (Grant No. 406964/2018-1), the Coordination for the Improvement of Higher Education Personnel, the National Institute of Science and Technology Complex Fluids, and the São Paulo Research Foundation (Grant No. 2014/50983-3).

[1] K. Adlem, M. Čopič, G. R. Luckhurst, A. Mertelj, O. Parri, R. M. Richardson, B. D. Snow, B. A. Timimi, R. P. Tuffin, and D. Wilkes, Phys. Rev. E **88**, 022503 (2013).

[2] M. Cestari, S. Diez-Berart, D. A. Dunmur, A. Ferrarini, M. R. de la Fuente, D. J. B. Jackson, D. O. Lopez, G. R. Luckhurst, M. A. Perez-Jubindo, R. M. Richardson *et al.*, Phys. Rev. E **84**, 031704 (2011).

[3] V. Borshch, Y.-K. Kim, J. Xiang, M. Gao, A. Jákli, V. P. Panov, J. K. Vij, C. T. Imrie, M.-G. Tamba, G. H. Mehl *et al.*, Nat. Commun. **4**, 2635 (2013).

[4] D. Chen, J. H. Porada, J. B. Hooper, A. Klittnick, Y. Q. Shen, M. R. Tuchband, E. Korblova, D. Bedrov, D. M. Walba, M. A. Glaser *et al.*, Proc. Natl. Acad. Sci. USA **110**, 15931 (2013).

[5] D. A. Paterson, J. P. Abberley, W. T. A. Harrison, J. M. D. Storey, and C. T. Imrie, Liq. Cryst. **44**, 127 (2017).

[6] J. P. Abberley, S. M. Jansze, R. Walker, D. A. Paterson, P. A. Henderson, A. T. M. Marcelis, J. M. D. Storey, and C. T. Imrie, Liq. Cryst. **44**, 68 (2017).

[7] Y. Wang, G. Singh, D. M. Agra-Kooijman, M. Gao, H. K. Bisoyi, C. Xue, M. R. Fisch, S. Kumar, and Q. Li, CrystEngComm **17**, 2778 (2015).

[8] D. Chen, M. Nakata, R. Shao, M. R. Tuchband, M. Shuai, U. Baumeister, W. Weissflog, D. M. Walba, M. A. Glaser, J. E. Maclennan *et al.*, Phys. Rev. E **89**, 022506 (2014).

[9] C. T. Archbold, E. J. Davis, R. J. Mandle, S. J. Cowling, and J. W. Goodby, Soft Matter **11**, 7547 (2015).

[10] R. J. Mandle, Soft Matter **12**, 7883 (2016).

[11] C. Zhu, M. R. Tuchband, A. Young, M. Shuai, A. Scarbrough, D. M. Walba, J. E. Maclennan, C. Wang, A. Hexemer, and N. A. Clark, Phys. Rev. Lett. **116**, 147803 (2016).

[12] Z. Parsouzi, S. M. Shamid, V. Borshch, P. K. Challa, A. R. Baldwin, M. G. Tamba, C. Welch, G. H. Mehl, J. T. Gleeson, A. Jakli, O. D. Lavrentovich, D. W. Allender, J. V. Selinger, and S. Sprunt, Phys. Rev. X **6**, 021041 (2016).

[13] M. Salamończyk, N. Vaupotič, D. Pociecha, C. Wang, C. Zhu, and E. Gorecka, Soft Matter **13**, 6694 (2017).

[14] P. K. Challa, V. Borshch, O. Parri, C. T. Imrie, S. N. Sprunt, J. T. Gleeson, O. D. Lavrentovich, and A. Jákli, Phys. Rev. E **89**, 060501(R) (2014).

[15] C. Meyer, G. R. Luckhurst, and I. Dozov, Phys. Rev. Lett. **111**, 067801 (2013).

[16] W. D. Stevenson, H.-X. Zou, X.-B. Zeng, C. Welch, G. Ungar, and G. H. Mehl, Phys. Chem. Chem. Phys. **20**, 25268 (2018).

[17] R. R. de Almeida, L. Evangelista, E. Lenzi, R. Zola, and A. Jákli, Commun. Nonlinear Sci. Numer. Simul. **70**, 248 (2019).

[18] Y. Wang, Z.-G. Zheng, H. K. Bisoyi, K. G. Gutierrez-Cuevas, L. Wang, R. S. Zola, and Q. Li, Mater. Horiz. **3**, 442 (2016).

[19] J. Xiang, Y. Li, Q. Li, D. A. Paterson, J. M. D. Storey, C. T. Imrie, and O. D. Lavrentovich, Adv. Mater. **27**, 3014 (2015).

[20] S. K. Prasad, P. L. Madhuri, P. Satapathy, and C. V. Yelamaggad, Appl. Phys. Lett. **112**, 253701 (2018).

[21] R. You, D. A. Paterson, J. M. D. Storey, C. T. Imrie, and D. K. Yoon, Liq. Cryst. **44**, 168 (2017).

[22] R. B. Meyer, in *Structural Problems in Liquid Crystals*, edited by R. Balian and G. Weill, Proceedings of the Les Houches Summer School of Theoretical Physics, XXV, 1973 (Gordon and Breach, New York, 1976), p. 273.

[23] R. B. Meyer, Phys. Rev. Lett. **22**, 918 (1969).

[24] I. Dozov, Europhys. Lett. **56**, 247 (2001).

[25] E. G. Virga, Phys. Rev. E **89**, 052502 (2014).

[26] G. Barbero, L. R. Evangelista, M. P. Rosseto, R. S. Zola, and I. Lelidis, Phys. Rev. E **92**, 030501(R) (2015).

[27] R. S. Zola, G. Barbero, I. Lelidis, M. P. Rosseto, and L. R. Evangelista, Liq. Cryst. **44**, 24 (2017).

[28] E. I. Kats, Low Temp. Phys. **43**, 5 (2017).

[29] J. A. Reyes, M. P. Rosseto, L. R. Evangelista, R. R. R. de Almeida, and R. S. Zola, Mol. Cryst. Liq. Cryst. **657**, 72 (2017).

[30] A. G. Vanakaras and D. J. Photinos, Soft Matter **12**, 2208 (2016).

[31] S. M. Shamid, S. Dhakal, and J. V. Selinger, Phys. Rev. E **87**, 052503 (2013).

[32] N. Vaupotič, M. Čepič, M. A. Osipov, and E. Gorecka, Phys. Rev. E **89**, 030501(R) (2014).

[33] N. Vaupotič, S. Curk, M. A. Osipov, M. Čepič, H. Takezoe, and E. Gorecka, Phys. Rev. E **93**, 022704 (2016).

[34] C. Meyer and I. Dozov, Soft Matter **12**, 574 (2016).

[35] I. Dozov and C. Meyer, Liq. Cryst. **44**, 4 (2017).

[36] S. V. Shiyanovskii, P. S. Simonário, and E. G. Virga, Liq. Cryst. **44**, 31 (2017).

[37] L. Radzihovsky and T. C. Lubensky, Phys. Rev. E **83**, 051701 (2011).

[38] P. G. de Gennes and J. Prost, *The Physics of Liquid Crystals* (Oxford University Press, New York, 1993).

[39] T. C. Lubensky, Phys. Rev. A **6**, 452 (1972).

[40] M. P. Rosseto, R. R. Ribeiro de Almeida, R. S. Zola, G. Barbero, I. Lelidis, and L. R. Evangelista, J. Mol. Liq. **267**, 266 (2018).

[41] C. Meyer, G. R. Luckhurst, and I. Dozov, J. Mater. Chem. C **3**, 318 (2015).

[42] S. Chandrasekhar, *Liquid Crystals* (Cambridge University Press, New York, 1992).

[43] O. D. Lavrentovich, P. Pasini, C. Zannoni, and S. Zumer, *Defects in Liquid Crystals: Computer Simulations, Theory and Experiments* (Springer Science + Business Media, New York, 2012).

[44] S. M. Salili, C. Kim, S. Sprunt, J. T. Gleeson, O. Parri, and A. Jakli, RSC Adv. **4**, 57419 (2014).

[45] E. Gorecka, N. Vaupotič, A. Zep, D. Pociecha, J. Yoshioka, J. Yamamoto, and H. Takezoe, Angew. Chem. Int. Ed. **54**, 10155 (2015).

[46] C.-J. Yun, M. Vengatesan, J. K. Vij, and J.-K. Song, Appl. Phys. Lett. **106**, 173102 (2015).

[47] R. Ribeiro de Almeida, C. Zhang, O. Parri, S. Sprunt, and A. Jákli, Liq. Cryst. **41**, 1661 (2014).

[48] G. Barbero, L. R. Evangelista, and I. Lelidis, Phys. Rev. E **67**, 051708 (2003).

[49] C. Meyer, Liq. Cryst. **43**, 2144 (2016).

[50] O. D. Lavrentovich and D.-K. Yang, Phys. Rev. E **57**, R6269 (1998).

[51] G. Durand, Liq. Cryst. **14**, 159 (1993).